



# Intelligent energy management strategy of hybrid energy storage system for electric vehicle based on driving pattern recognition

Jie Hu <sup>a,b,c,\*</sup>, Di Liu <sup>a,b,c,\*\*</sup>, Changqing Du <sup>a,b,c</sup>, Fuwu Yan <sup>a,b,c</sup>, Chen Lv <sup>d</sup>

<sup>a</sup> Hubei Key Laboratory of Advanced Technology for Automotive Components, Wuhan University of Technology, Wuhan 430070, China

<sup>b</sup> Hubei Collaborative Innovation Center for Automotive Components Technology, Wuhan University of Technology, Wuhan 430070, China

<sup>c</sup> Hubei Research Center for New Energy & Intelligent Connected Vehicle, Wuhan University of Technology, Wuhan 430070, China

<sup>d</sup> School of Mechanical and Aerospace Engineering, Nanyang Technological University, 639798, Singapore

## ARTICLE INFO

### Article history:

Received 7 June 2019

Received in revised form

29 October 2019

Accepted 1 March 2020

Available online 3 March 2020

### Keywords:

Hybrid energy storage system

Driving patterns recognition

Transient power

Adaptive wavelet transform

Fuzzy logic control

## ABSTRACT

To achieve optimal power distribution of hybrid energy storage system composed of batteries and supercapacitors in electric vehicles, an adaptive wavelet transform-fuzzy logic control energy management strategy based on driving pattern recognition (DPR) is proposed in view of the fact that driving cycle greatly affects the performance of EMS. The DPR uses cluster analysis to classify driving cycles into different patterns according to the features extracted from the historical driving data sampling window and utilizes pattern recognition to identify real-time driving patterns. After recognition results are obtained, an adaptive wavelet transform is employed to allocate the high frequency components of power demand to supercapacitor which contains transient power and rapid variations, while the low frequency components are distributed to battery accordingly. The use of fuzzy logic control is to maintain the SOC of supercapacitor within desired level. The simulation results indicate that the proposed control strategy can effectively decrease the maximum charge/discharge current of battery by 58.2%, and improve the battery lifetime by 6.16% and the vehicle endurance range by 11.06% compared with conventional control strategies. Further demonstrate the advantage of hybrid energy storage system and the presented energy management strategy.

© 2020 Elsevier Ltd. All rights reserved.

## 1. Introduction

### 1.1. Background and motivation

With the energy crisis and environmental pollution, electric vehicles (EVs) are considered as a promising alternative transportation tool compared to conventional internal-combustion-engine vehicles due to its excellent performance of high efficiency and low pollutant emission [1,2]. Battery is widely in EVs for their high energy density. However, batteries used in EVs often encounter instantaneous power demands, thus they tend to perform frequent charge/discharge operations, which will result in

the breakdown of electrochemical structure and pose adverse effect on battery lifespan [3,4]. Moreover, the EVs demand both high energy and high power densities of the onboard energy storage system, but batteries have comparatively high energy density yet low power density. One effective solution to this issue is the adoption of hybrid energy storage systems (HESS) composed of battery and supercapacitor. Supercapacitors have higher power density, longer cycle life and faster charge/discharge performance, which is quite suitable to serve as an auxiliary energy source in EVs to satisfy the instantaneous high power requirements [5,6]. Therefore, the problem faced by single battery with low power density or supercapacitor with low energy density can be well solved by combining energy sources with different density characteristics [7–9]. In order to meet the vehicle requirements including demand power, safety and reliability, the development of energy management system (EMS) and design of the power distribution strategy are critical for HESS.

\* Corresponding author. Hubei Key Laboratory of Advanced Technology for Automotive Components (Wuhan University of Technology), Wuhan, 430070, China.

\*\* Corresponding author. Hubei Key Laboratory of Advanced Technology for Automotive Components (Wuhan University of Technology), Wuhan, 430070, China.

E-mail addresses: [auto\\_hj@163.com](mailto:auto_hj@163.com) (J. Hu), [liudi1710@163.com](mailto:liudi1710@163.com) (D. Liu).

## 1.2. Literature of exiting EMS

To achieve optimal power distribution of HESS a variety of EMS are proposed, it can be generally classified into rule-based and optimization-based strategies. Rule-based strategies have been widely used for their simple implementation and high computational efficiency. The rules are roughly categorized into deterministic rules and fuzzy rules. Deterministic rules include logic threshold and filter control. An integrated rule-based meta-heuristic optimization approach was used to deal with a multi-level EMS of a multi-source EV for sharing energy and power between battery and supercapacitor in [10]. Zeng et al. [11] put forward a power allocation strategy based on wavelet transform. The original power demand signal is decomposed by wavelet transform into high frequency and low frequency components, which are allotted to the supercapacitor and battery respectively according to their output characteristics. Fuzzy rules are based on fuzzy logic control, including conventional and optimized fuzzy controllers [12,13], to distribute power between different sources. In [13], a fuzzy logic controller optimized by golden cut-off rule was proposed and simulation results have shown the method can effectively realize the design objective set forth.

Optimization-based strategies are broadly classified into global optimization and real-time optimization. The EMS is designed by minimizing the chosen cost function subject to the specified constraints. Common cost functions include equivalent fuel consumption [14], life cycle [15] cost and battery energy loss [16]. Global optimization includes dynamic programming (DP), genetic algorithm (GA) and Convex optimization, while real-time optimization contains model predictive control (MPC) and Pontryagin's Minimum Principle. Song et al. [17] utilized DP to deal with the integrated optimization problem and obtain the best configuration and energy split strategies of HESS in an electric city bus. In [18], the parameters of the EMS were optimized by GA and Pareto front analysis in a framework of multi-objective optimization. Song et al. [19] formulated a fast parameter matching method for HESS. The HESS parameters and corresponding EMS are optimized simultaneously by convex optimization theory. An adaptive optimal power splitting EMS for fuel-cell/battery hybrid system was proposed in [20], and the online optimization problem based on the Pontryagin's Minimum Principle was developed to minimize hydrogen consumption. Borhan et al. [21] adopted MPC strategy to split power between the combustion engine and electrical machines, and it shows a noticeable improvement in fuel economy with respect to other controls.

The key issue with HESS is how to effectively protect the battery by using the SC. However, one drawback to these EMS is their computational cost for on-line implementation. More important, most of the existing control strategies have focused on the optimization of the EMS based on a fixed driving cycle, which utilizes the same optimized parameters for different driving cycles. The underlying influence of various driving cycles is commonly neglected. Due to the complexity and variability traffic environments, the power demand of vehicular system usually contains peak power and high transient power, which will pose tremendous pressure to the battery in EVs. Therefore, taking the influence of driving cycle into consideration is critical when developing the EMS to the safety, longevity and cost of the HESS.

## 1.3. Original contribution

To the best of our knowledge, there are few papers considering the influence of changeable driving cycles on EMS for HESS, which will obtain better control performance with a prior knowledge of driving cycles. It has become one of the research hotspots to fusion

traffic information into the EMS of hybrid electric vehicles (HEVs). Advanced location technology such as global positioning systems and intelligent transport systems are already used to obtain driving information to improve the performance of EMS [21,22]. Moreover, the EMS based on optimization can hardly be used in real time for the high dependency on driving cycles and online computational complexity. Therefore, to address this issue, this study proposes an intelligent EMS for HESS on the premise of considering driving cycle and computational complexity. The following original contributions make this paper different from aforementioned work.

The presented strategy consists of three modules, namely DPR module, wavelet transform module and fuzzy control module. Firstly, fuzzy c-means (FCM) cluster analysis is used to classify driving cycles into different patterns off-line and the driving pattern is distinguished by pattern recognition in real-time. The DPR is the basis of adaptive wavelet transform, which aims at improving the adaptivity of EMS to driving cycles. Secondly, the wavelet transform is adopted in EMS for its excellent performance in transient power recognition [23,24]. The wavelet transform module dynamically adjusts the decomposition level of wavelet transform according to the recognition result. The high frequency and low frequency components of the power demand generated by wavelet transform are allocated to supercapacitor and battery respectively. Thirdly, despite the advantage of wavelet transform in recognizing transient power, it can't monitor and maintain the SOC of supercapacitor in real-time. The supercapacitor SOC should be maintained within an appropriate range to improve energy saving, the supercapacitor bank should have enough energy stored to supply peak power and sufficient capacity to recover breaking energy. Thus, fuzzy logic control is adopted to maintain the SOC of supercapacitor within the desired level due to its flexibility and robustness [25,26]. Finally, a simulation based on MATLAB/Simulink is conducted under test driving cycle to verify the effectiveness of proposed strategy for HESS. The results indicate that the presented EMS shows rationality in terms of extending battery lifespan and improving system efficiency and driving range. Compared with a single ESS, the proposed strategy can improve the battery service life by 6.16% and driving range by 11.06%.

## 1.4. Outline of the paper

The remainder of this paper is organized as follows. Section 2 gives the topology and model frameworks of the HESS. Section 3 illustrates the method of DPR. Section 4 details the proposed intelligent EMS of adaptive wavelet transform-fuzzy logic control based on DPR. The verification and evaluation of proposed EMS are conducted in Section 5. Conclusions are given in Section 6.

## 2. System description and modeling

### 2.1. Structure of the HESS

A hybrid energy storage system comprising battery and supercapacitor achieves long battery life and good power and energy performance when there are significant power swings and energy regeneration, which is true for EVs operating in various traffic environments [27]. The batteries can be charged from the grid and provide sufficient energy for electric drives, whereas the SCs can store the peak power to extend the battery life [28]. As for the HESS topologies, there are many designs for its configurations, including passive, active, and semi-active with different power electronics. The optimization results in reference [29] show that the semi-active HESS offers a good balance between performance and system cost. Hence, a typical semi-active HESS is adopted in this study as shown in Fig. 1. A bi-directional DC/DC converter is used to

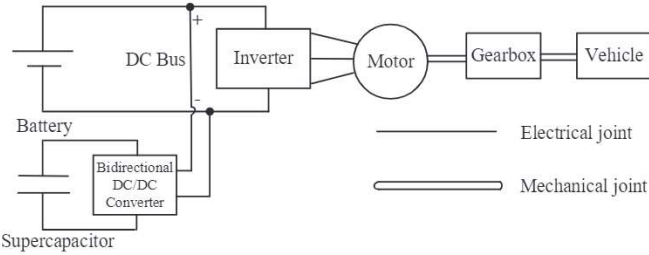


**Fig. 1.** Structure of hybrid energy storage system.

interface the supercapacitor with battery/DC Bus, and a inverter is connected to the motor.

## 2.2. Battery model

The battery model is presented by the Rint model in this study as shown in Fig. 2 (a).  $U_{bat}$  and  $I_{bat}$  represent the battery open-voltage and current respectively.  $R_{bat}$  is inner resistance.

Since the relationship between remaining capacity and voltage is nonlinear in batteries, therefore SOC is adopted to indicate the remaining capacitor of battery in the current state. It's defined as the ratio of residual capacity  $C_r$  to the maximum available capacity  $C_{max}$ , and can be calculated by using the ampere-hour counting method. The definition of SOC and calculation of the ampere-hour counting method are as follows [30]:

$$SOC_{bat} = \frac{C_r}{C_{max}} = \frac{C_r - \eta \int_0^t I_{bat} dt}{C_{max}} \quad (1)$$

Where  $\eta$  represents the charge and discharge efficiency of battery.

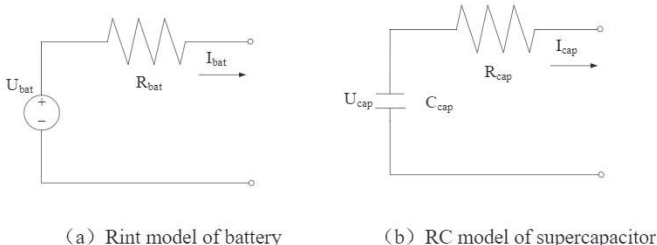
## 2.3. Supercapacitor model

Fig. 2(b) shows the classical RC model of Supercapacitor used mostly in literature.  $C_{cap}$  and  $R_{cap}$  represent the supercapacitor capacity and inner resistance.  $U_{cap}$  and  $I_{cap}$  is the supercapacitor open-voltage and current respectively.

For supercapacitors, the relationship between remaining capacity and terminal voltage is more linear, thus the SOC of supercapacitor is used to indicate the remaining capacity, it can be expressed as [30]:

$$SOC_{cap} = \frac{U_{ter} - U_{min}}{U_{max} - U_{min}} \quad (2)$$

Where  $U_{ter}$  represent the supercapacitor terminal voltage,  $U_{min}$  and  $U_{max}$  are the minimal and maximal cut-off voltage of supercapacitor respectively.



**Fig. 2.** Model of battery and supercapacitor.

## 2.4. DC/DC converter

The function of bidirectional DC/DC converter is to distribute power according to the voltage regulation between battery and supercapacitor, so that the HESS can operate normally. In essence, it's a switch, hence the efficiency model is adopted to represent the DC/DC converter in this section. The efficiency  $\eta$  can be described:

$$\eta = f\left(\frac{U_{bat}}{U_{cap}}, P\right) \quad (3)$$

Where  $f\left(\frac{U_{bat}}{U_{cap}}, P\right)$  is a look-up table function which take battery voltage and supercapacitor voltage ratio as input, and  $P$  represents the input power of DC/DC converter.

According to the above model analysis, the semi-active HESS simulation model is established based on the built-in electric vehicle model in ADVIASOR, which is an advanced vehicle simulation software developed in MATLAB/Simulink. The basic parameters of the vehicle and HESS are listed in Tables 1 and 2 respectively.

## 3. Driving pattern recognition

Driving cycle is significantly important to vehicle systems, such as vehicle power system matching [31], EMS formulation [32] and EV range estimation [33]. Therefore, with the acquirement of driving cycles, a variety of vehicle functions can be improved. Zhang et al. used fuzzy logic to classify typical driving cycles into different patterns and identify the real-time driving pattern, and the proposed EMS based on DPR indicates better fuel efficiency than conventional controls [34]. Additionally, many intelligent algorithms such as learning vector quantization [35], Supported vector machine [36], artificial neural network [37] are also utilized to identify the driving patterns. Thus, the influence of driving cycles on EMS is considered in this paper, and the DPR method used is described as follows.

### 3.1. Selection of characteristic parameters

The vehicle driving segments are divided by the method of fixed step, which is set to 100s per segment, and the NYCC driving cycle is used to illustrate the division in Fig. 3. Based on this division method, 25 typical driving cycles are selected and divided into 200 driving segments. For a determinate driving cycle, the number of description parameters can be as high as 62 [38]. Too many parameters increase recognition difficulty, while too few parameters lead to inaccurate identification. In literature [39,40], the characteristic parameters of driving cycles are average velocity, average running velocity, maximum velocity, maximum acceleration, maximum deceleration, average acceleration, percentage of idling, percentage of accelerating, percentage of decelerating, percentage of constant velocity, total mileage and standard deviation of acceleration. The 12 parameters mentioned above are extracted from each segment to facilitate driving pattern recognition subsequently.

The principal component analysis (PCA) is conducted on these features to obtain the representative characteristic parameters which mainly reflect the driving patterns. The PCA results of characteristic parameters are 12 principal components represented by  $Y_i$  ( $i = 1, 2, \dots, 12$ ) as listed in Table 3. The principal components corresponding to the cumulative contribution rate above 80% are usually selected to represent all the original variables for analysis to achieve dimension reduction. Meanwhile, the selection of principal component usually requires the eigenvalue to be more than 1 [40]. Therefore, the first four principal components  $Y_1$ ,  $Y_2$ ,  $Y_3$  and  $Y_4$  are selected. Then, the representative characteristic parameters are

**Table 1**  
Basic parameters of vehicle.

vehicle parameters	
Windward area	2.19 m <sup>2</sup>
Tire radius	0.262 m
Air resistance coefficient	0.32
Rolling resistance coefficient	0.02
Efficiency of the transmission system	0.96

**Table 2**  
Basic parameters of HESS.

Components parameters		
Battery	Battery type	NI-MH battery
	Nominal voltage/V	12
	Nominal capacity/Ah	90
	Number of cells	27
Supercapacitor	Supercapacitor type	Maxwell PC2500
	Nominal voltage/V	2.7
	Nominal capacity/F	1000
	Number of cells	119

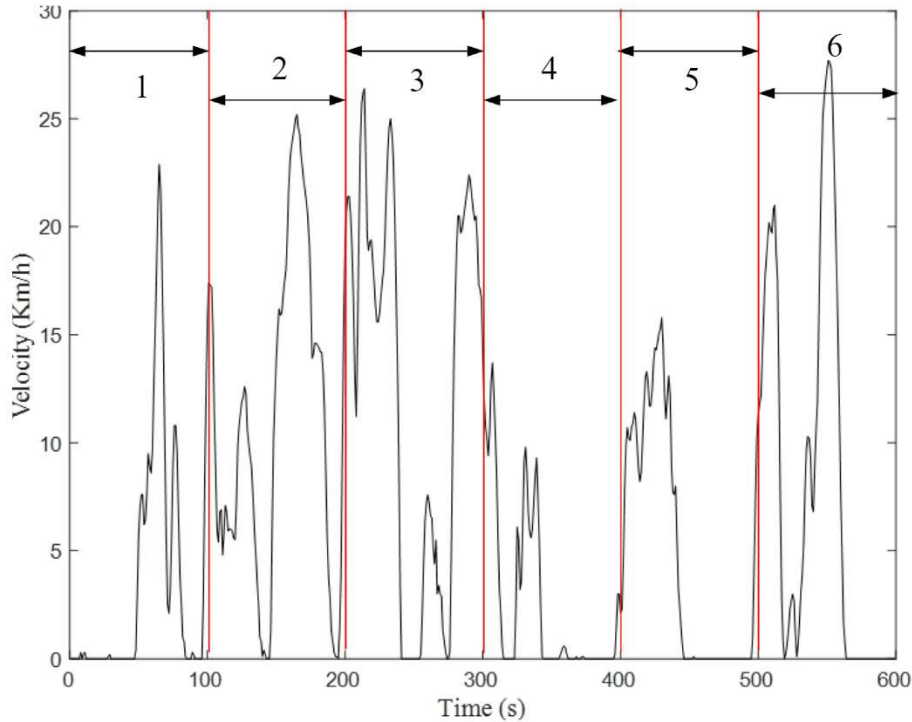


**Fig. 3.** Division of driving segments.

chosen based on the correlation between the characteristic parameters and the first four principal components. They are average velocity, percentage of idling, percentage of decelerating and percentage of constant velocity.

### 3.2. FCM cluster analysis

Cluster analysis is a common classification method, whose purpose is to divide the objects to be classified into several categories according to certain rules. FCM cluster analysis is adopted to classify these driving segments into different patterns in this section.

In cluster analysis, the selection of the number of categories is

significant, which is presented by as letter C in this section. If the number of categories is too small, it will be hard to classify accurately, while too many categories will increase the recognition difficulty. Considering the actual driving conditions, the minimum and maximum value of C is 3 and 5 respectively. Fig. 4 compares the classification centers of different clusters. It's clear that if C = 3, the time proportion of each pattern is obviously different and the classification is reasonable. While C = 4 and 5, the time proportion difference is not obvious in the deceleration state, so the driving cycles is classified into three patterns.

The classification results are further analyzed, the idling time percentage and average velocity are chosen to delineate different clusters and the classification centers are marked in Fig. 5. The

**Table 3**

Results of principal component analysis.

principal components	eigenvalue	Variance contribution rate	Cumulative contribution
Y1	4.895	40.792	40.792
Y2	2.456	20.463	61.255
Y3	1.391	11.589	72.844
Y4	1.169	9.740	82.583
Y5	0.637	5.306	87.889
Y6	0.599	4.996	92.885
Y7	0.459	3.822	96.707
Y8	0.326	2.718	99.425
Y9	0.062	0.517	99.942
Y10	0.007	0.058	100.000
Y11	$5.672 \times 10^{-6}$	$4.727 \times 10^{-5}$	100.000
Y12	$3.566 \times 10^{-16}$	$2.972 \times 10^{-15}$	100.000

coordinate of category 1 is (12.13, 0.376). The idling proportion is high and the average velocity is low, it represents the urban congestion in this case. The coordinate of category 3 is (99.60, 0.007), the idling proportion is low and the average velocity is high, which represents the highway pattern. The coordinate of category 2 is (42.21, 0.083), the idling proportion and average velocity is between the urban congestion and the highway, it represents the suburban environment. Therefore, the driving patterns are roughly classified into three typical patterns, namely urban congestion, suburb, highway. The classification result is consistent with the actual driving condition, it can be considered as a reasonable classification.

### 3.3. Driving pattern recognition

The DPR is based on the assumption that the driving pattern will not change suddenly in a short period. Therefore, the DPR module can predict future driving patterns in real-time through the analysis of the past sampling data within a short time window.  $\Delta T$  and  $\Delta t$  represents the length of sampling time window and predicting time window. In Fig. 6, the historical driving cycle data in the time range from  $t - \Delta T$  to  $t$  is collected as data set to predict future  $\Delta t$  time range driving pattern, and  $\Delta T = 150$ s and  $\Delta t = 5$ s obtain more accurate results [41].

The DPR module collects the historical driving cycle data by sampling time window. It then processes these data and establishes the feature vectors denoted as B, which consist of the representative characteristic parameters.  $A_n(n = 1, 2, 3)$  represents the feature vectors of three typical driving patterns, namely the central coordinate of each cluster. The Euclidean distance is adopted to calculates the distance between the feature vector sampled from the real-world driving cycles and standard feature vectors of the three driving patterns. The distance between vectors  $A_n$  and B is calculated by the Euclidean distance  $\sigma(A_n, B)$  as follows [32].

$$\sigma\left(A_n, B\right)=1-\frac{1}{\sqrt{m}}\left(\sum_{k=1}^m A_n k-B(k)\right)^2 \quad (4)$$

where  $m$  is the number of characteristic parameters.

The module selects one of the reference driving patterns with the most similarity as the recognition result, namely the maximum  $\sigma$  values from an array of  $3\sigma$  values as fellows.

$$\sigma(B, A_n)=\max \{\sigma(B, A_1), \sigma(B, A_2), \cdots, \sigma(B, A_n)\} \quad (5)$$

In order to verify the effectiveness of DPR method, some typical driving cycles that selected from the standard driving cycle library in ADVISOR are randomly combined as the test driving cycle. It's

composed of typical urbancongestion, suburb and highway (NYCC + INDIA\_URBAN + US06 + REP05). The recognition result of test driving cycle shows in Fig. 7. It's indicate that the proposed DPR can effectively identify the driving patterns of test driving cycle combined randomly in real-time.

### 3.4. EMS of adaptive wavelet transform-fuzzy control based on DPR

To fulfill the power allocation of the demand power and energy sources including the battery and supercapacitor under different driving cycles, an intelligent EMS based on DPR is proposed in this section.

### 3.5. Wavelet transform algorithm

As mentioned earlier, the power demand of vehicle contains various sharp peaks and transients, which would shorten the battery lifetime. The wavelet transform is a powerful tool in the analysis of power transient phenomena because of its ability to extract information from the transient signals simultaneously in the time and frequency domain. It can decompose a given signal into components with different positions and scales [42].

Wavelet transform (WT) is mainly used in the aspect of fault diagnosis [43], signal processing [44] and image recognition [45] in automobile previously. It has also been used in EMS recently for its excellent performance in transient power recognition [46,47], which can isolate the base power demand from transients. The transients can be extracted from the total power by wavelet transform and delivered to the supercapacitor, since the charge/discharge time of supercapacitor can vary from several milliseconds to minutes. Zhang [48] creatively introduced wavelet transform into the EMS of HESS and results show the battery can effectively avoid transient power and extend the fuel-cell lifespan. A combination between wavelet transform and neural network was developed in [49]. The neural network serves as a controller determining the requested power from fuel-cell. The wavelet transforms of a given signal  $s(t)$  is:

$$W(\lambda, u)=\int_R s(t) \frac{1}{\sqrt{\lambda}} \psi\left(\frac{t-u}{\lambda}\right) d t \quad (6)$$

Where  $s(t)$  is the original signal,  $\lambda$  is the scaling factor,  $\psi$  is the mother wavelet function and  $u$  is the translation factor.

Haar wavelet has the shortest filtering length in the time domain and is also the simplest among all the wavelets. It has a nice feature that its forward and inverse transform are the same, which is convenient for signal processing and improves the code execution efficiency [50]. Therefore, the Haar wavelet is selected as mother wavelet. Fig. 8 illustrates the process of decomposition and

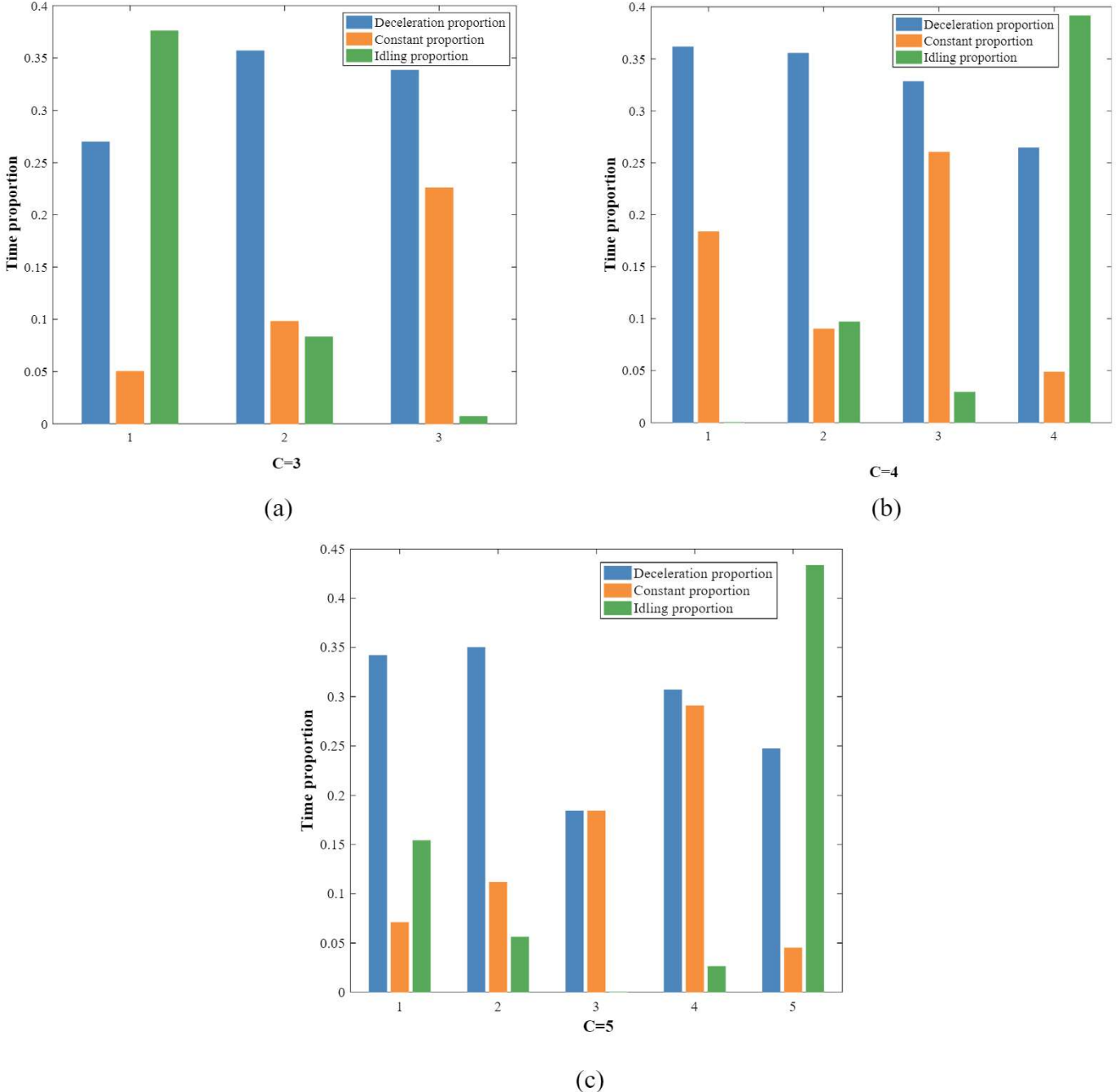


**Fig. 4.** Cluster centers with different C values.

reconstruction of given signal  $s(t)$  using a three-level Haar WT. The original signal is decomposed by a high-low pass filter  $[H_1(z), H_0(z)]$  and reconstructed by a reconstruction filter  $[G_1(z), G_0(z)]^T$  step by step. Taking the load required power as the input  $s(t)$ , with the usage of three-level Haar WT, the low frequency components  $s_0(t)$  and high frequency components  $(s_1(t) + s_2(t) + s_3(t))$  of power demand can be separated effectively, which are distributed to battery and supercapacitor respectively.

### 3.6. Sliding windows

The existing EMS based on WT usually processes data offline. In order to process the power demand signal in real time, a

rectangular sliding window is added before WT. The sliding window is used to collect signals, since a single signal can't be filtered [51]. Every time the signal is sampled, the system outputs the filtered signal correspondingly. During the filtering process, a window of fixed length is used to move in the same time period to intercept a segment of the power signal sequence. The WT of collected signals is implemented by Mallat algorithm, which requires  $2^j$  data ( $j \in N^+$ ) for WT. Thus, the amount of collected signals in sliding window should also be  $2^j$ . The basic idea of real-time WT as follows [51]. It is assumed that the obtained real-time signal sequence at time  $k$  is  $a_1, a_2, \dots, a_k$ . If  $k < 2^j$ , the amount of data collected in sliding window doesn't meet the requirement. WT is not conducted and the output is  $a_k$  at that moment. If  $k = 2^j$ , the

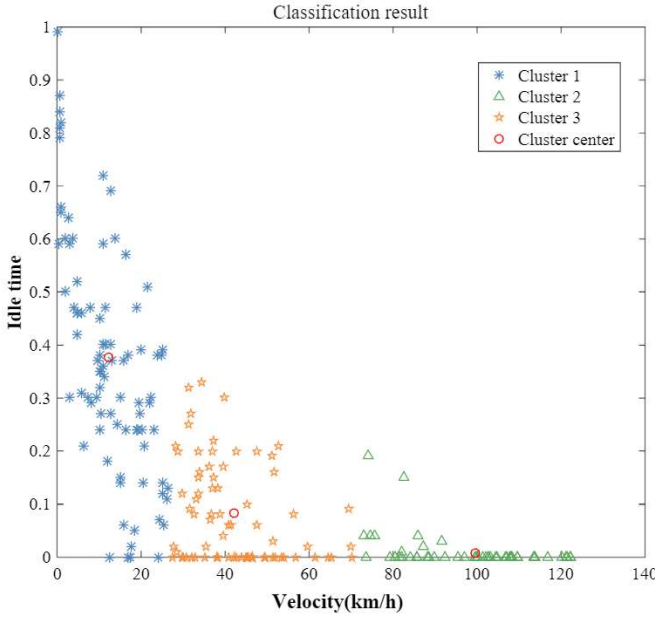


**Fig. 5.** Classification results of driving segments.

amount of data exactly satisfies the requirements. The data collected in sliding window is processed by WT for the first time and the output is the last value after filtering. If  $k > 2^j$ , the WT of collected data is continuously conducted and the last value obtained by filtering is used as output. Fig. 9 shows the moving process of sliding window. In general, if the decomposition level of WT is  $L$  and the length of sliding window is  $W$ , the relationship between them must satisfy the inequation  $W \geq 2^j$ . If the length of sliding window is too short, the filtering effect is not obvious. While the filtering time is too long to ensure the filtering speed if the sliding window is very long. WT performs better filtering effect when  $W = 32$  [51], therefore, the length of sliding window is 32.

### 3.7. Selection of decomposition level

For EMS based on WT, the selection of decomposition level is critical. The previous application of wavelet transform is arbitrary

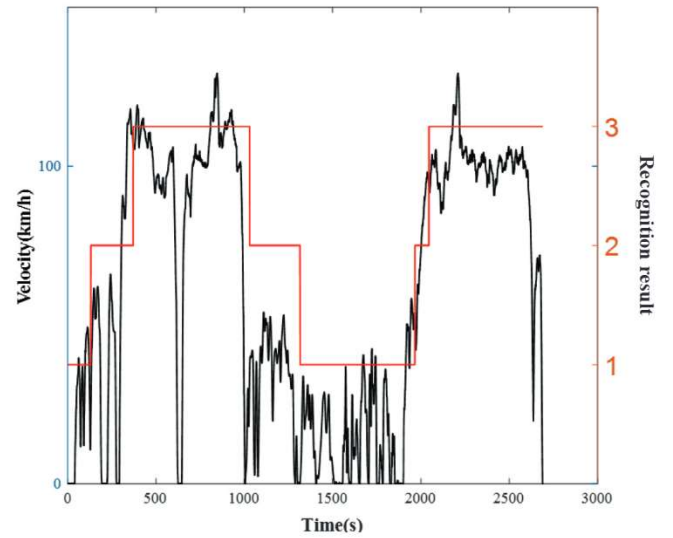


**Fig. 7.** The recognition result of test driving cycle.

when choosing the mother wavelet and decomposition level. If the inherent frequencies of energy sources are not considered when utilizing WT, it will result in the battery operating in unhealthy condition and reducing the lifespan of related power source. Let  $f_s$  be the sampling frequency of vehicle power signal and  $f_c$  be the upper frequency limit of low frequency power signal. Therefore, if the decomposition level is  $L$ , they must verify the following condition [52]:

$$L = \left\lfloor \frac{\log\left(\frac{f_s}{f_c}\right)}{\log 2} - 1 \right\rfloor \quad (7)$$

where  $\lfloor \cdot \rfloor$  is the inferior integer part.

Since the frequency interval for battery is  $[10^{-2}, 10^{-1}]$  Hz, the system sample frequency is 1Hz [52]. From Eq. (7), it can be computed that the decomposed level interval is  $2 \leq L \leq 5$ . If the decomposition level  $L$  and the length of sliding window satisfy the inequation  $W \geq 2 \cdot 2^L$ , WT has better filter reconstruction effect

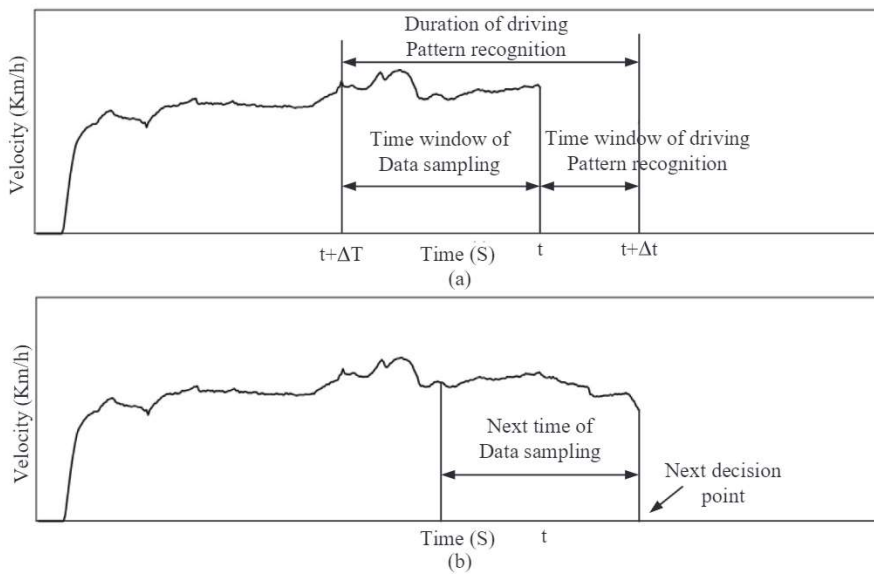


**Fig. 6.** Schematic diagram of driving pattern recognition.

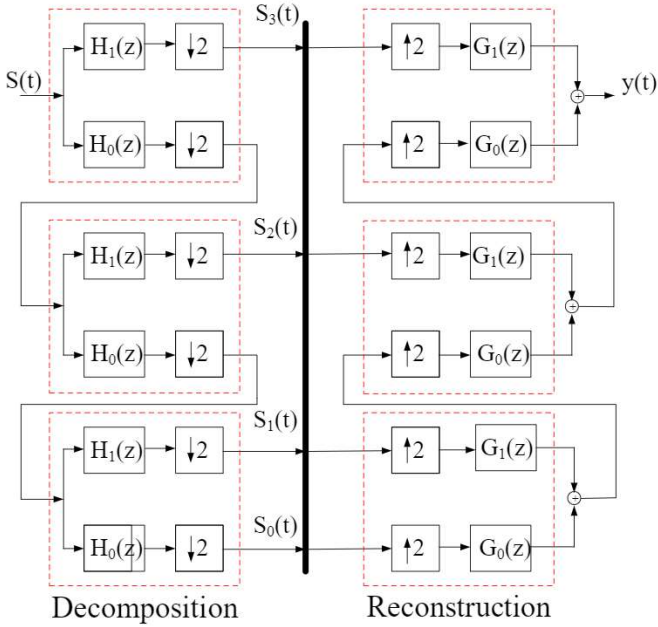


**Fig. 8.** The model of decomposition and reconstruction using wavelet transform.

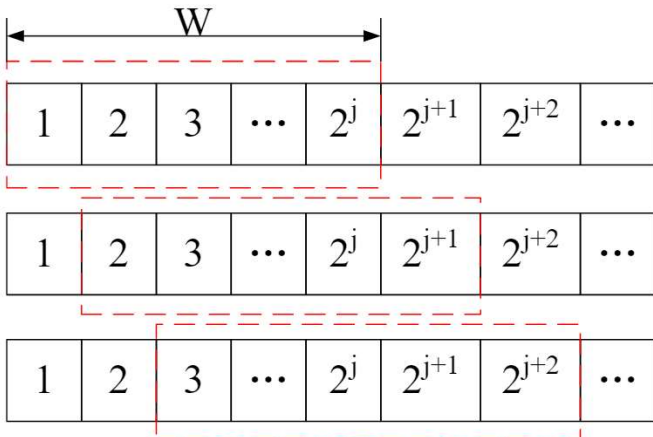


**Fig. 9.** The moving process of sliding window.

[51]. Therefore, the maximum decomposition level is adjusted to be 4, and the available WT decomposition levels are 2, 3 and 4.

Considering the existing EMS based on WT mostly adopts fixed decomposition level, namely a sole frequency decomposition, an intelligent adaptive wavelet transform based on DPR is proposed. It's able to select the corresponding decomposition level based on the recognition result. From congestion cycle to highway cycle, the power demand signal and high-frequency interference signal increase correspondingly as the velocity increases. Thus, the decomposition level 2, 3 and 4 correspond to urban congestion cycle, suburban cycle and highway cycle respectively. This correspondence can limit the output power of battery within appropriate range. It can not only avoid the large charge/discharge current of battery, but also reduce battery voltage fluctuation and temperature rise, which is beneficial to extend the battery lifetime.

### 3.8. Fuzzy logic control

As mentioned earlier, in order to ensure all the energy sources

operate in appropriate range, the supercapacitor bank should have enough energy stored to supply peak power when the vehicle is accelerating or climbing and have sufficient capacity to recover breaking energy [53]. As one of the important branches of intelligent control, fuzzy logic control has been widely used in control, signal processing, communication and other fields [54], which is also very suitable for the control of HEVs for its own flexibility and robustness [25,26]. Consequently, fuzzy logic control is introduced to maintain the supercapacitor SOC within an appropriate level. The energy  $E_{cap}$  stored in supercapacitor can be computed as follows:

$$E_{cap} = \frac{1}{2} U_{cap}^2 C_{cap} \quad (8)$$

$E_{cap\_max}$  is denoted as the maximum energy stored in supercapacitor when supercapacitor is fully charged, at this time the voltage is  $U_{cap\_max}$  and SOC is 1. In other cases, if  $U_{cap}$  is 1/2 of  $U_{cap\_max}$ , it means the SOC is 0.5 and  $E_{cap}$  is merely 1/4 of  $E_{cap\_max}$ . It's not sufficient to supply peak power demand. Besides, the supercapacitor efficiency is quite low in the low SOC region [55], thus the lower threshold of supercapacitor SOC is 0.5. If  $U_{cap}$  is 0.7 of  $U_{cap\_max}$ , namely the SOC is 0.7 and the  $E_{cap}$  is nearly 1/2 of  $E_{cap\_max}$ . It means that the supercapacitor can supply the power demand during the accelerating periods and have available capacity to capture the breaking energy. Consequently, the ideal value of supercapacitor SOC is 0.7 in this section.

The operation modes of HESS in EVs are mainly divided into drive and regenerative braking mode. Considering the differences in power demand and control focus under these two modes, fuzzy controllers for them are formulated respectively as shown in Fig. 10. The input is the reference output power of battery, the SOC of battery and supercapacitor, while the output is the actual output power of battery. The reference output power of battery is the low frequency components of power demand generated by wavelet transform. If the SOC value of supercapacitor is around 0.7, the battery supplies the reference value. However, if the SOC value of supercapacitor is lower than 0.7, the battery provides more power than the reference to increase the energy stored in supercapacitor. Similarly, if the SOC of supercapacitor is higher than 0.7, the battery delivers power that appropriately smaller than the reference. Therefore, the supercapacitor SOC can be kept within an appropriate range [53]. The output surface of fuzzy rules is presented in Fig. 11.

Simply utilizing WT or fuzzy control alone to distribute power of HESS has its disadvantages. Conventional fuzzy logic control can't decompose different components of power demand effectively according to the dynamic response characteristics of energy sources, while wavelet transform can't maintain the SOC of supercapacitor within an appropriate range, both of which neglect the

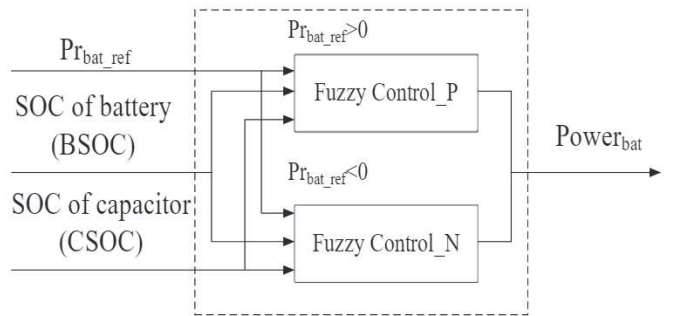


**Fig. 10.** Model of fuzzy logic control.

influence of driving cycles on EMS. Therefore, an adaptive wavelet transform-fuzzy logic control EMS based on DPR is proposed to address this issue, the frame of the proposed EMS shows in Fig. 12.

#### 4. Results and discussion

In order to verify the effectiveness of proposed EMS for HESS, the simulation is conducted based on the established MATLAB/Simulink model under test driving cycle and the results is discussed in this section.

##### 4.1. Comparison of battery in different ESS

The simulation results of different ESS in EV are illustrated in Fig. 13. Compared with a single ESS with battery, the SOC of battery in HESS declines more slowly due to the introduction of supercapacitor. The high frequency components extracted from the total power are distributed to the supercapacitor, which alleviates the peak power demand of loads on battery during acceleration and braking. In Fig. 13 (b), (c) and (d), battery in the HESS is less impacted by large charge/discharge currents. Furthermore, the voltage fluctuation and power amplitude of battery are also smaller, which are conducive to extending the battery cycle life. Therefore, the advantages of HESS are significantly obvious compared with a single ESS.

##### 4.2. Comparison of battery and supercapacitor in the HESS with different WT

Fig. 14 shows the comparison results of WT with different levels in HESS. Compared with conventional WT with a fixed decomposition level, the adaptive WT based on DPR has better performances in adaptability. In Fig. 14(a), the SOC of battery with adaptive WT decreases more slowly. On account of introducing adaptive WT with DPR, the power distribution between battery and supercapacitor is dynamically adjusted according to the recognition results. Low frequency components with relatively smooth variation in power demand are allocated to battery, thus the fluctuation of battery SOC is smaller. While the high frequency components are distributed to supercapacitor, whose SOC changes with the variation of high frequency components correspondingly as shown in Fig. 15(a).

Besides, Fig. 14(b) shows the charge/discharge current of battery with different EMS, and it's obvious that the proposed adaptive WT can adaptively reduce the charge/discharge current compared with other strategies. The large peak current is taken by supercapacitor as shown in Fig. 15 (b), whose characteristics of quick charge/discharge are utilized adequately. Moreover, it can be seen from the enlarged image of Fig. 14(b), there are three curves from 2550s to

2611s, and another three different curves from 2611s to 2630s. This is because the recognition result of the DPR module is highway in time range from 2550s to 2611s, at this time the curve of adaptive WT is overlap with the curve of 4-level WT. Similarly, the recognition result is suburban in the time range from 2611s to 2630s, so the curve of adaptive WT is overlap with another one. This indicates that the presented EMS shows great adaptability to different driving cycles.

##### 4.3. Comparison of different ESS with different control strategies

The comparison results of battery in different ESS are illustrated in Fig. 16. Compared with single ESS and HESS based on adaptive WT, the SOC of battery in HESS with adaptive WT-FLC declines more slowly in Fig. 16(a). The reason can be further analyzed from Figs. 16(d) and 18(a). On the one hand, owing to the introduction of adaptive WT, the smoothed low frequency components of the power demand is supplied by battery. On the other hand, fuzzy logic control is adopted to maintain the SOC of supercapacitor in pre-defined limits to raise the efficiency of HESS. If the supercapacitor SOC is very high, the battery output power can be appropriately reduced. Thus, the battery SOC consumption is saved effectively.

In Table 4, the strategy A and B represent the strategy of adaptive WT and adaptive WT - FLC in HESS respectively. It can be seen from Table 4 that compared with the battery in single ESS, the energy utilization rates in HESS with strategy A and B improve by 5.97% and 8.9%. Furthermore, the battery SOC consumption in HESS with control strategy A has saved 0.017, namely the saved energy is 0.488 kW·h. Meanwhile, the energy consumed by supercapacitor is 0.006 kW·h, so the energy saved is 0.482 kW·h, which is enough to maintain the vehicle at a constant velocity of 60 km/h for 4.823 km. Similarly, the energy saved in the HESS with strategy B is enough for the vehicle to drive at a constant velocity of 60 km/h for 5.08 km. The extend range have improved about 11.06% compared with the whole mileage of test driving cycle (45.93 km).

The operating current distribution of different ESS shows in Fig. 17. The phenomenon of large discharge current of battery in single ESS is more obvious in Fig. 17(a), while the discharge rate of battery in HESS is mainly less than 1C. The discharge current distribution of battery in HESS is more concentrated, which is conducive to maintain battery healthy state. In Fig. 17(b), the supercapacitor in HESS with control strategy B supplies more of the large current by contrast of startegy A. what's more, the distribution of supercapacitor current in the large current region of strategy B is greater than that of strategy A, which can reduces the impact of large current on battery effectively.

Figs. 16 (b) and 18 (a) shows the charge/discharge current of battery in different ESS with different strategies. The discharge current of battery in single ESS exceeds 180A partly, meanwhile the discharge rate of battery is greater than 2C, which is harmful to battery health [56]. By contrast, the discharge current of battery in HESS with adaptive WT-FLC is largely within 100A, and the discharge rate is far less than 2C. The battery's maximum discharge current in single ESS is 244.6A, while the values in HESS with adaptive WT and adaptive WT-FLC are 112.3A and 102.2 A respectively. Compared with the conventional single ESS, the maximum discharge current of battery reduced by 50% and 58.2%.

The voltage comparison of battery in different systems can be observed clearly in Figs. 16(c) and 18(b). Among all the simulation results, battery voltage fluctuation based on the proposed control strategy is the smallest. For one thing, the fluctuation of low frequency components extracted from power demand via adaptive WT itself is smooth. For another thing, the battery output power is slightly lower than the reference value when the supercapacitor SOC is higher than 0.7, so the battery voltage fluctuation is smaller.

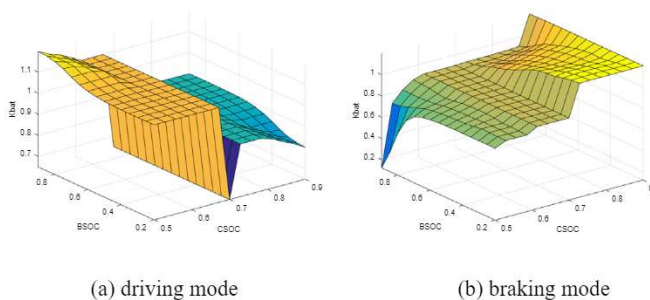
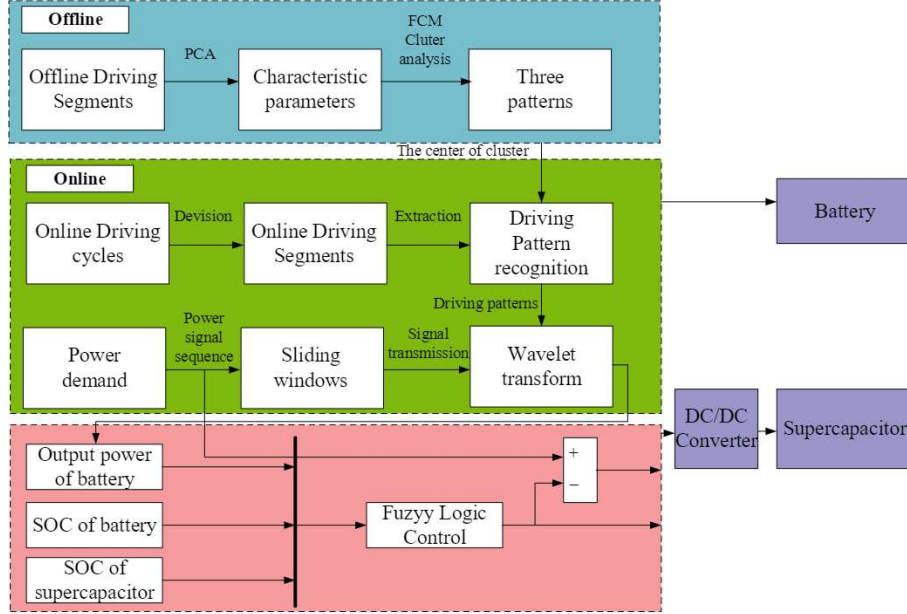


Fig. 11. Fuzzy rules output surface.



**Fig. 12.** Frame of proposed EMS.

The output voltage of battery with the adaptive WT-FLC fluctuates within the interval [307V,330V], whose maximum voltage drop is 23V. For a battery pack comprised by 27 battery cells in series, the average voltage fluctuation is 0.85V per battery cell, reduces by 56.6% compared with 1.96V voltage fluctuation in a single ESS. Smaller voltage fluctuation of battery cell can reduce the inconsistency between battery connected in series, improve the energy utilization of battery and extend its lifetime [57].

Fig. 19(a) represents the variation of supercapacitor SOC in HESS with different EMS. It's evident that the supercapacitor SOC based on the proposed strategy changes more dramatically. After the simulation, the supercapacitor SOC still remains around 0.7, which indicates the effectiveness of proposed strategy. On the one hand, the supercapacitor SOC can be successfully maintained around the desired level. At this moment the capacity of supercapacitor is sufficient to recuperate braking energy, and supercapacitor bank stores enough energy to supply the required load power when the vehicle is accelerating or climbing. On the other hand, if the supercapacitor SOC is higher than the predefined value, the energy stored and recuperated from braking can also be used to save battery SOC consumption, it's beneficial to extending EV driving range.

The operating temperature of battery in different ESS is illustrated in Fig. 20. The battery temperature in single ESS rises faster and the maximum rising value is 2.75 °C, while the rising value in HESS is only 1.94 °C, and the temperature rise decreases by 29.5%. The battery operating under high temperature conditions frequently will shorten its life [58]. The introduction of supercapacitor in HESS reduces the operating temperature for battery significantly, it contributes to prolonging battery lifetime.

Figs. 21 and 22 show the discharging and charging efficiency of battery in different ESS under a certain driving cycle. It's clearly that the discharging efficiency of battery has significantly improved in HESS compared with single ESS, which is mainly concentrated in the high efficiency range. In addition, the number of battery charging state point is remarkably reduced in HESS. This is because the supercapacitor in HESS has recovered most of the energy during

regenerative braking, which reduces the frequency of battery charging and the impact of large current posed on battery. Thus, the overall system efficiency is improved in HESS.

As the energy source of EVs, the battery is required a large number of charges and discharges to meet the power demand of different driving cycles. However, the service life of battery is limited.

Thus, the total operating cost of the EV is largely depend on the cycle numbers and replacement cost of battery [59]. In fact, due to the complexity and uncertainty of driving cycle, the battery of vehicle operates under highly dynamic conditions that do not match the cycle traditionally used by manufactures to characterize the lifespan in laboratory conditions [60]. Therefore, it's significant to estimate the battery life accurately.

A phenomenological battery life estimation model is adopted in this article. It based on a damage accumulation model that uses the concept of accumulated Ah-throughput (i.e. the total amount of electrical charge that can flow through the battery before it reaches the end of life), which depends on the actual operating conditions [60]. To evaluate the effective life depletion of the battery charge, the Ah-throughput is computed as:

$$Ah_{eff}(t) = \int_0^t \sigma |I(\tau)| d\tau \quad (9)$$

Where  $\sigma$  is the severity factor, it at the cell level depends on the C-rate ( $I_c$ ), temperature and depth of discharge (DOD). For charging-sustaining EVs/HEVs, the effect of the C-rate is the most important aging factor [60]. Therefore, a simplified severity factor with respect to the C-rate is considered in this paper, as follows:

$$\sigma = \frac{1.6}{625} (I_c)^2 + 1 \quad (10)$$

Where C-rate is an index defined as the ratio of the current (A) to the nominal charge capacity (Ah), and can be expressed as:

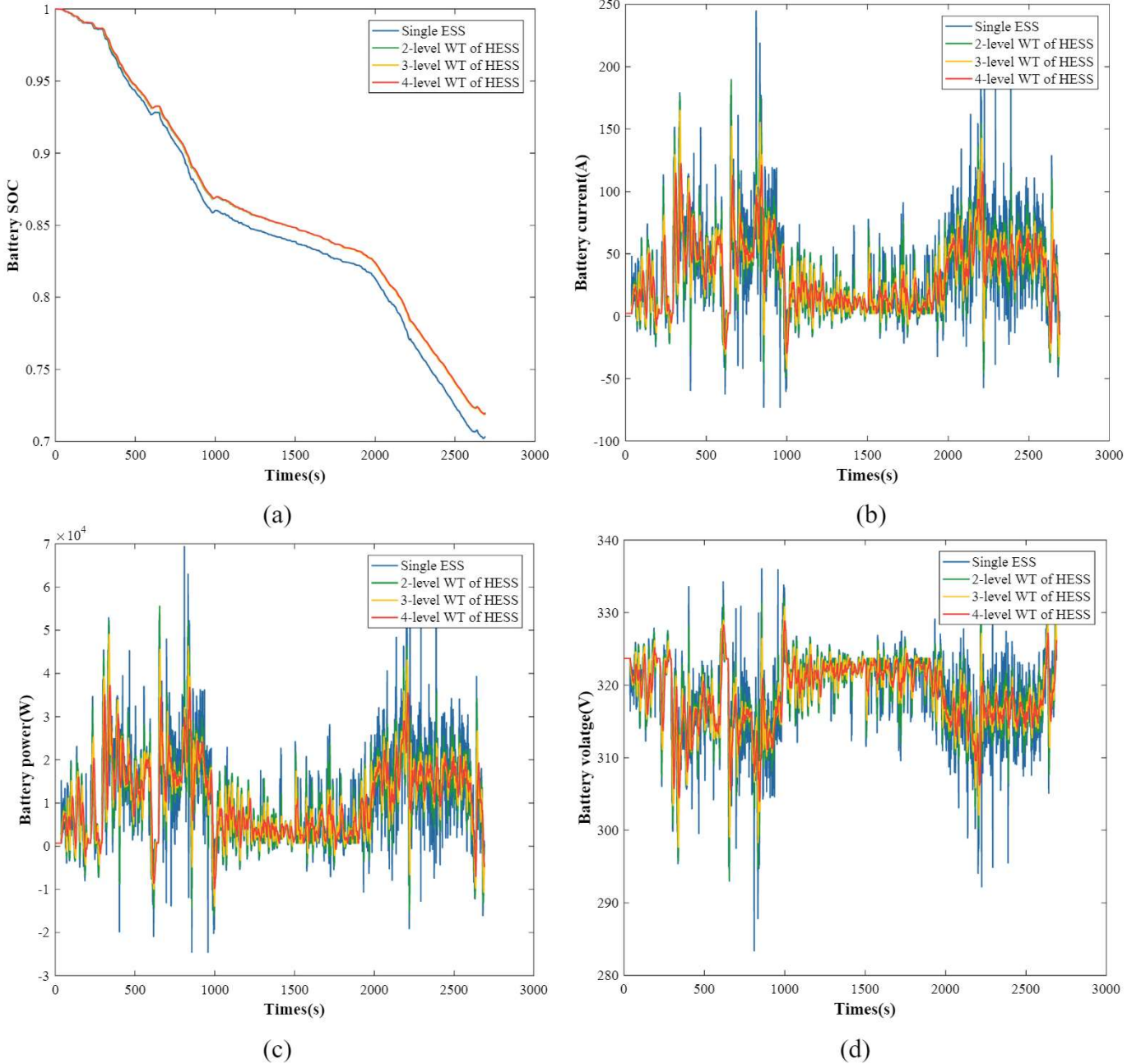


**Fig. 13.** The comparison of battery in different ESS. WT, wavelet transform.

$$I_c = \frac{I}{Q_{batt}} \quad (11)$$

The end of battery is reached when  $Ah_{eff} = \Gamma$ .  $\Gamma$  is the total Ah-throughput of battery, which is constant for a given battery. According to literature [60], the equivalent battery life is:

$$L = \frac{\Gamma}{Ah_{eff}} = \frac{20000 \times 3600 \times Q_{batt}}{2.3 \times Ah_{eff}} \quad (12)$$

Where L is the number of driving cycle that battery can service,  $Q_{batt}$  is the nominal battery capacity.

Therefore, from Eq. (12), the number of available cycles of battery in single ESS is 28688 under test driving cycle, while the number is 29753 and 30454 of battery in HESS with adaptive WT and adaptive WT-FLC, the battery service life improved 3.71% and 6.16% respectively.

## 5. Conclusions

This paper proposes an energy management strategy of adaptive wavelet transform-fuzzy logic control based on driving pattern recognition for HESS of EVs, which aims at addressing the receiving problem of transient power for battery when the EVs drive under

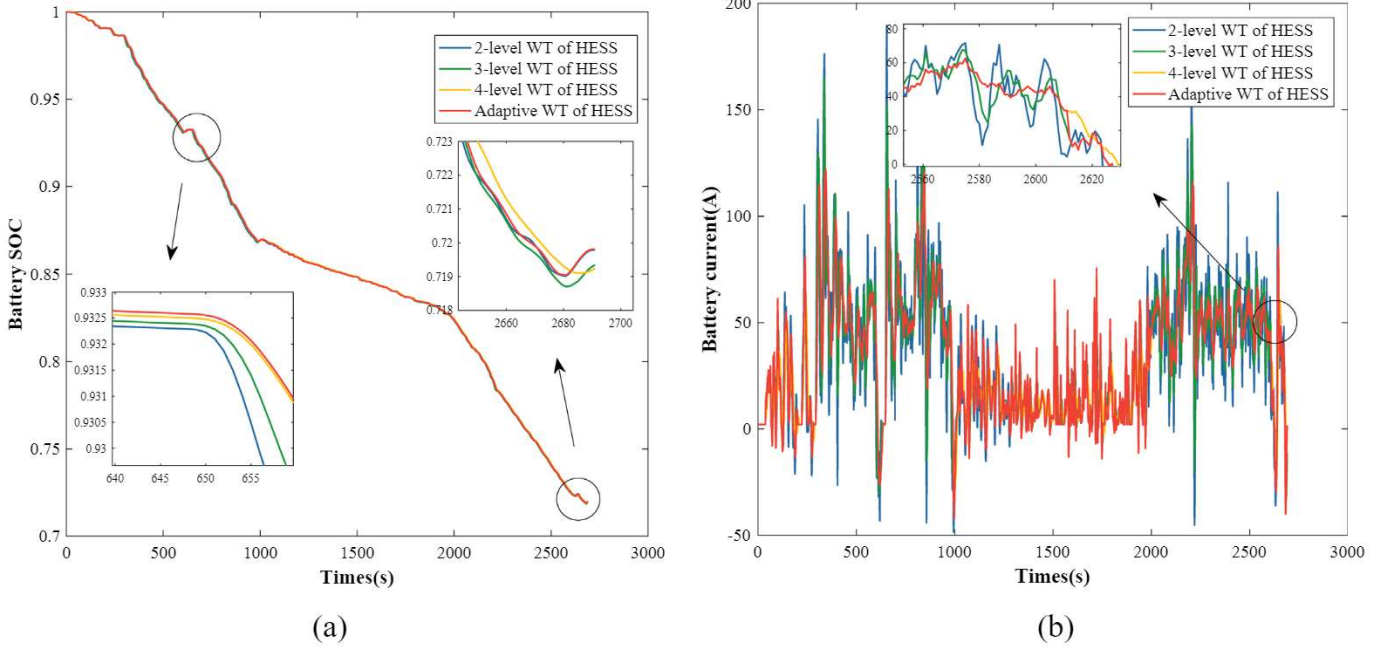


**Fig. 14.** The comparison of battery in the HESS with different strategy.

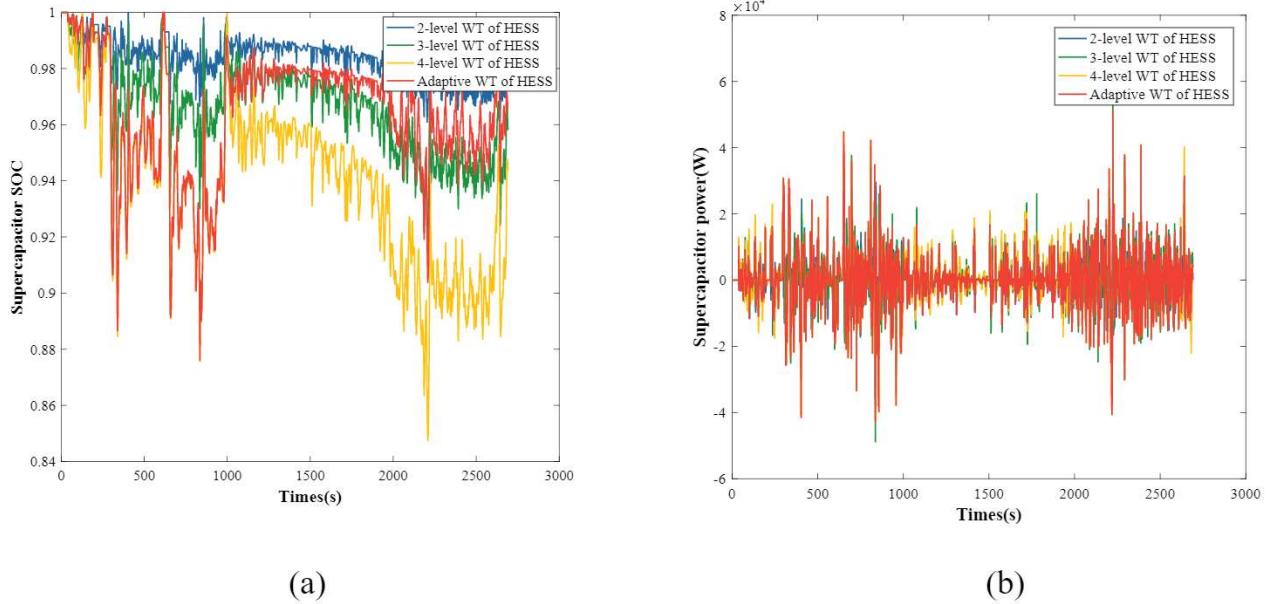


**Fig. 15.** The comparison of supercapacitor in the HESS with different strategy.

different driving cycles. A driving pattern recognition module has been adopted to distinguish the driving patterns in real-time, which can eliminate the impact of driving cycles on power allocation. An adaptive EMS based on the recognition results has been proposed by combining wavelet transform and fuzzy logic control together. The adaptive wavelet transform decomposes the power demand into different components that approximate the natural characteristic of energy sources. Besides, the SOC of supercapacitor is maintained within desired level by fuzzy logic control, which is convenient for supercapacitor to supply instantaneous peak power and capture breaking energy.

The simulation is conducted on MATLAB/Simulink based on test driving cycle to evaluate the performance of proposed control strategy. Simulation results indicate that the proposed strategy of HESS performs better flexibility, it can dynamically adjust the decomposition level of wavelet transform. Thus, the perturbations of charge/discharge current and voltage are diminished effectively. The maximum current and voltage fluctuation of battery in HESS remarkably reduced by 58.2% and 56.6% respectively when compared to conventional single ESS. In addition, the proposed strategy can also improve the battery service life by 6.16% and the extend range by 11.16%, it's conducive to reduce total operating

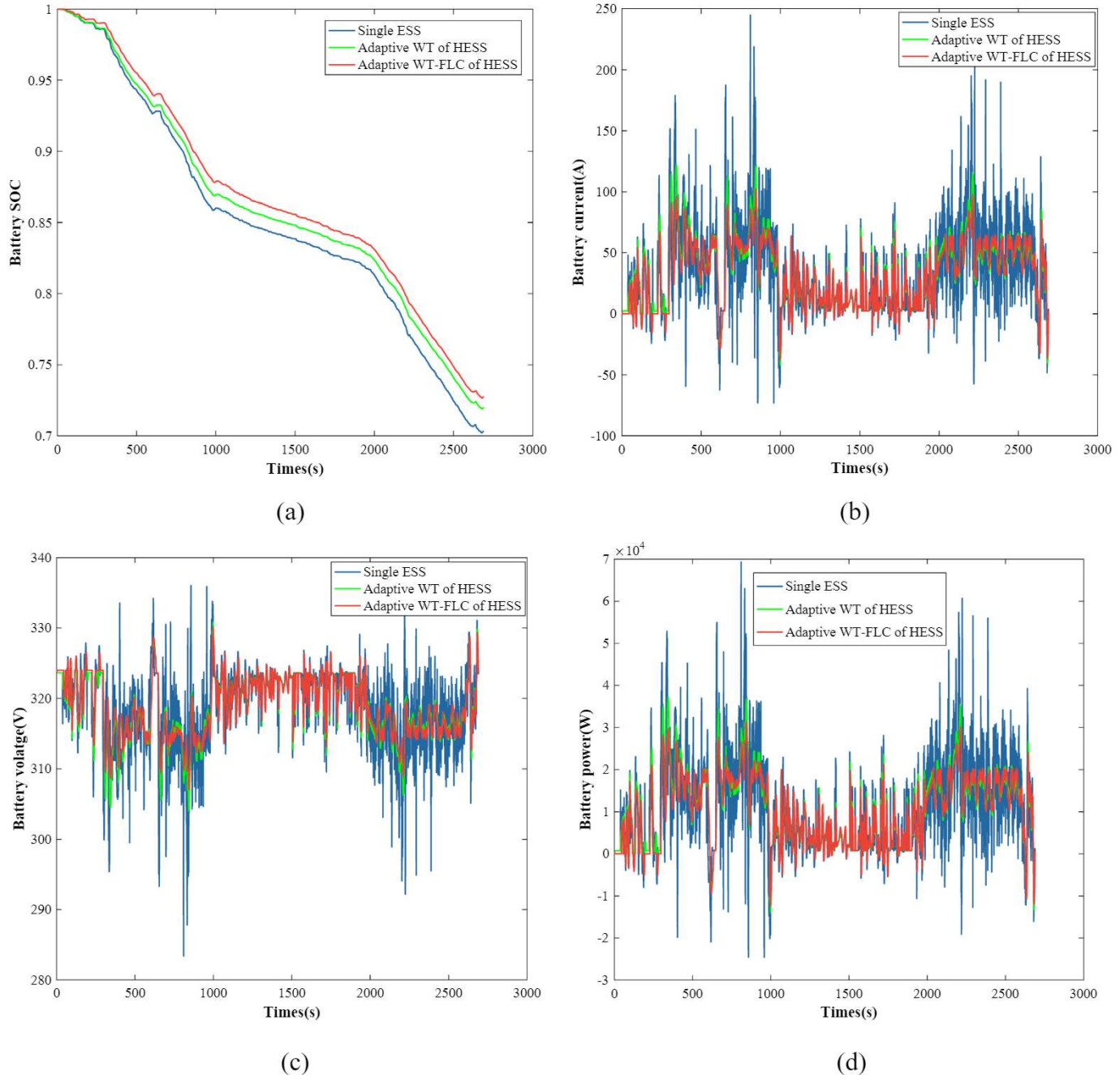


**Fig. 16.** Battery comparison in different ESS with different strategies. Adaptive WT-FLC, adaptive wavelet transform-fuzzy logic control.

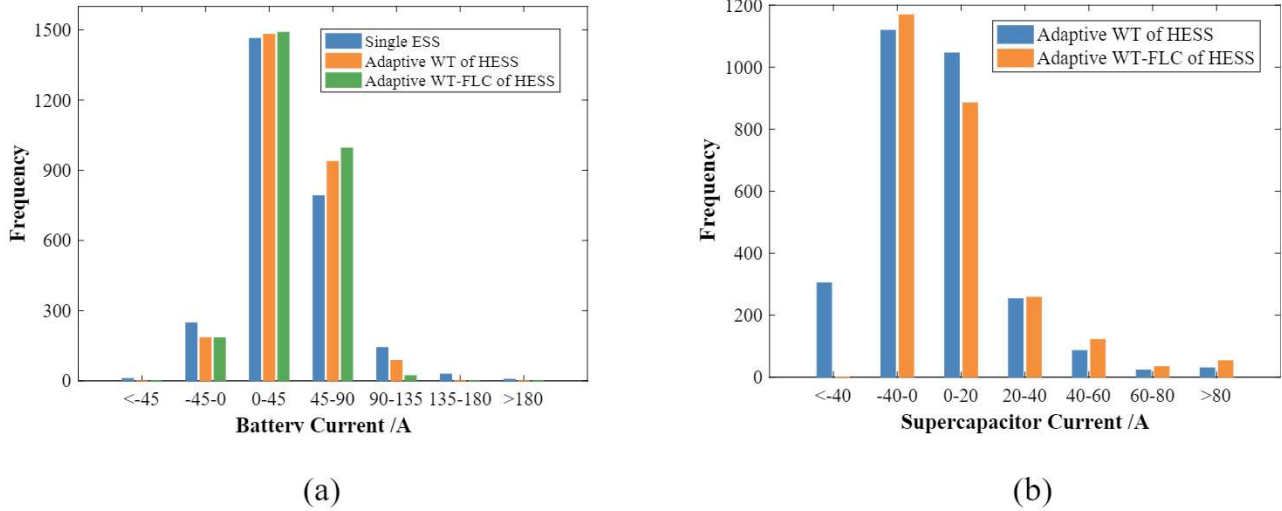


**Fig. 17.** The current distribution comparison in different ESS.

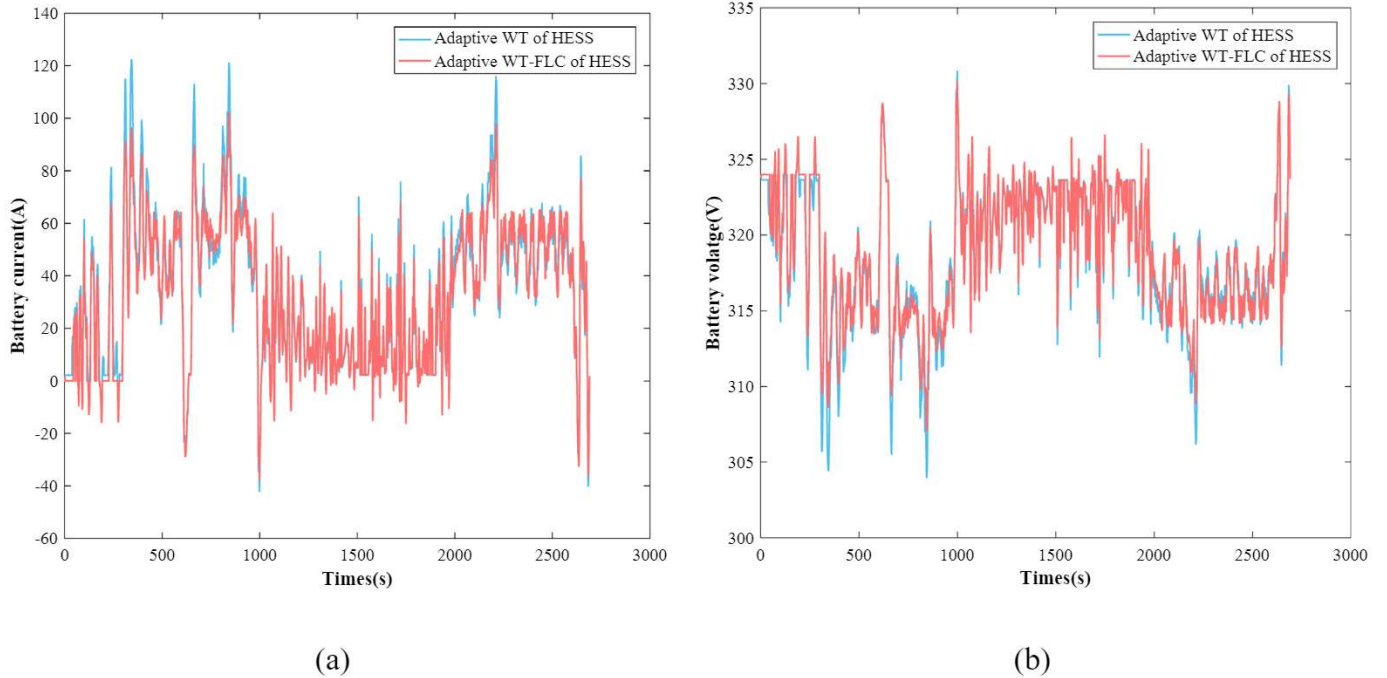


**Fig. 18.** The battery comparison in HESS with different control strategy.

**Table 4**

The comparison of battery SOC variation under test driving cycle.

Type System	Start SOC	End SOC	variation of SOC	Relative variation of SOC	Percentage
Single ESS	1	0.703085	0.296915	0	0
strategy A	1	0.719810	0.280190	0.016726	5.97%
strategy B	1	0.727362	0.272638	0.024278	8.90%

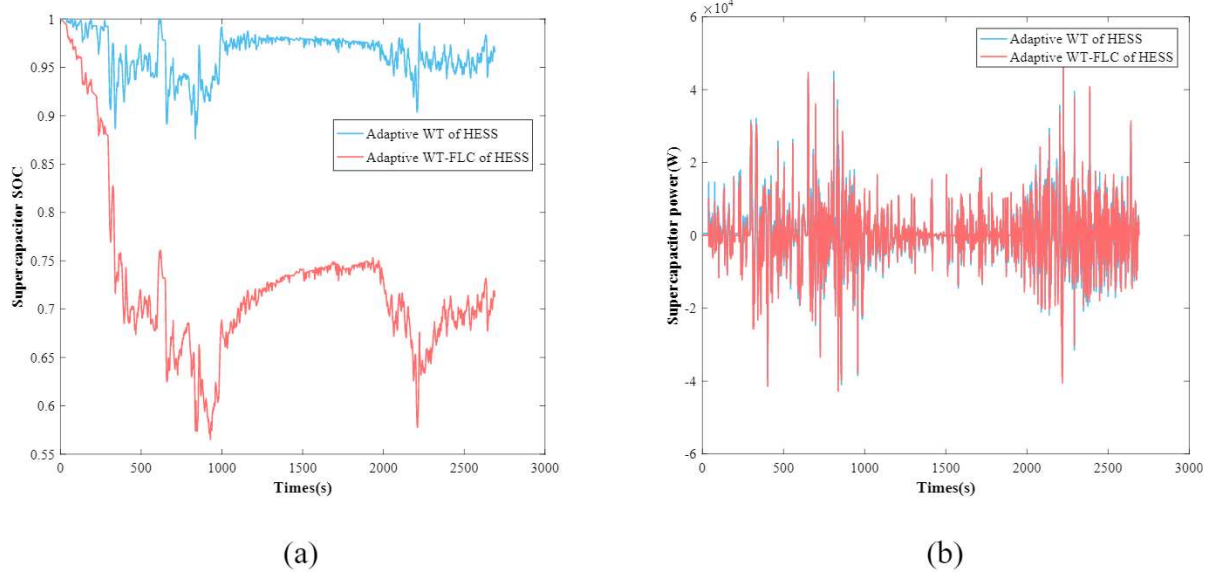


**Fig. 19.** The supercapacitor comparison in HESS with different EMS.

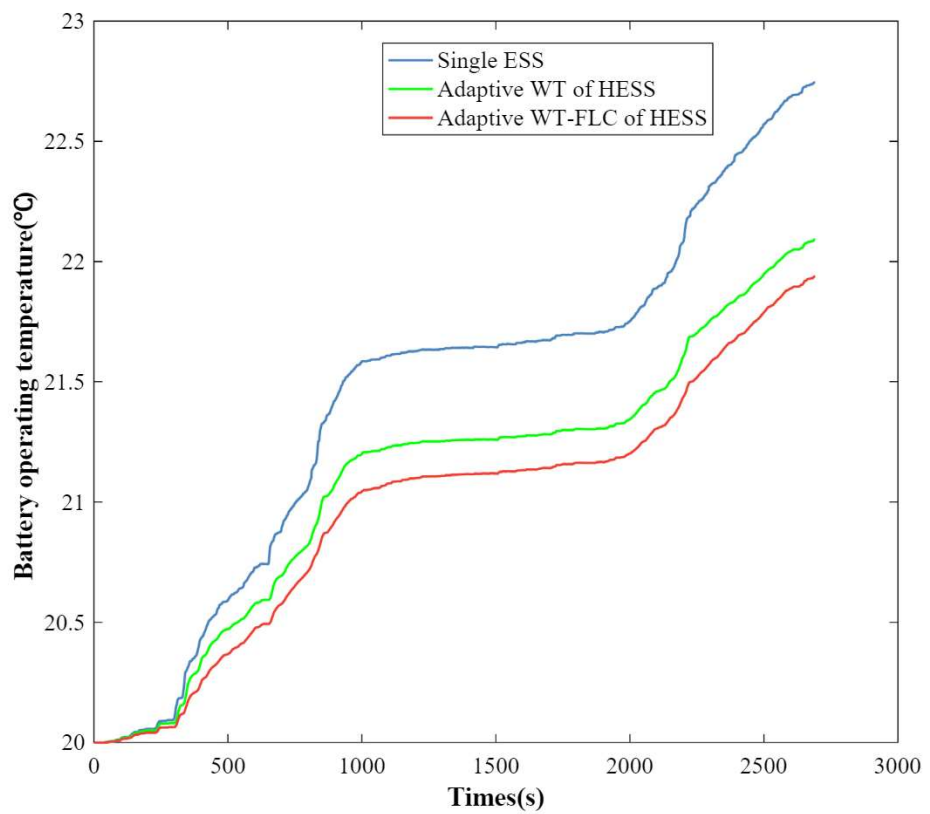


**Fig. 20.** Battery temperature comparison in different ESS.

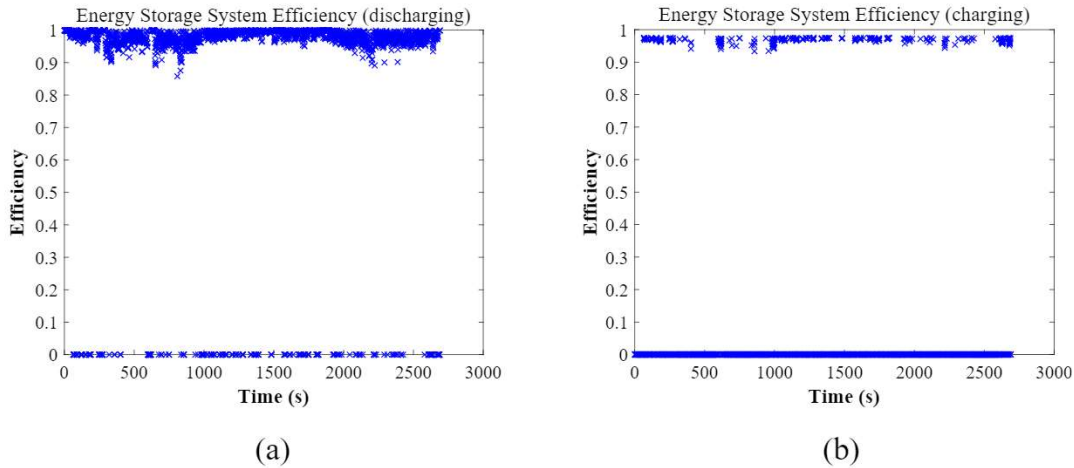


**Fig. 21.** The discharging and charging efficiency of battery in single ESS.

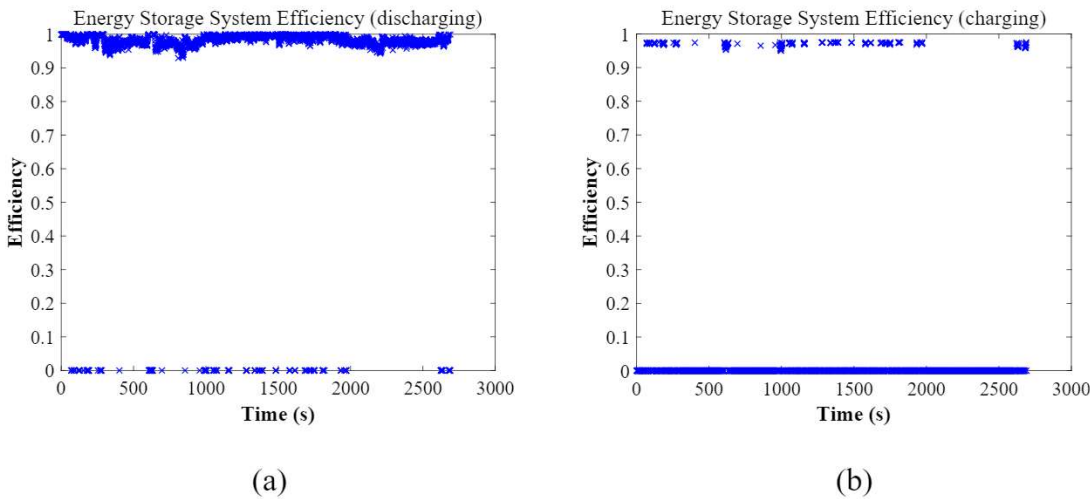


**Fig. 22.** The discharging and charging efficiency of battery in HESS.

cost of the EVs. Further researches will focus on designing an experiment to validate effectiveness of proposed energy management strategy by means of bench test.

## Acknowledgments

The authors wish to gratefully acknowledge the Hubei Key Laboratory of Advanced Technology for Automotive Components (Wuhan University of Technology, China). This study was financially supported by the National Natural Science Foundation (Grant No. 51775393), China, Liuzhou Science and Technology Planning Project (Grant No. 2018BC20501), China, Innovative Research Team Development Program of Ministry of Education of China (Grant No. IRT\_17R83), China and 111 Project (Grant No. B17034), China.

## References

- [1] Rade M, Dhamal SS. Battery-Ultracapacitor combination used as energy storage system in electric vehicle[C]//. In: 2015 international conference on emerging research in electronics, computer science and technology (ICERECT). IEEE; 2015.
- [2] Singh A, Pattnaik S. Design of an efficient power sharing strategy for a battery-ultracapacitor hybrid energy storage system[C]//. In: IEEE international conference on power electronics. IEEE; 2017.
- [3] Baisden A, Emadi A. ADVISOR-Based model of a battery and an ultra-capacitor energy source for hybrid electric vehicle. *IEEE Trans Veh Technol* 2004;53(1):199–205.
- [4] Song Z, Hofmann H, Li J. Energy management strategies comparison for electric vehicles with hybrid energy storage system. *Appl Energy* 2014;134:321–31.
- [5] Shen Khaligh A. Design and real-time controller implementation for a battery-ultracapacitor hybrid energy storage system[J]. *IEEE Trans Ind Inform* 2016;2:1910–8.
- [6] Camara MB, Gualous H, Gustin F. Design and new control of DC/DC converters to share energy between supercapacitors and batteries in hybrid vehicles[J]. *IEEE Trans Veh Technol* 2008;57(5):2721–35.
- [7] Hochgraf CG, Basco JK, Bohn TP. Effect of ultracapacitor-modified PHEV protocol on performance degradation in lithium-ion cells[J]. *J Power Sources* 2014;246:965–9.
- [8] Santucci A, Sorniotti A, Lekakou C. Power split strategies for hybrid energy storage systems for vehicular applications[J]. *J Power Sources* 2014;258:395–407.
- [9] Xiong R, Chen H, Wang C, et al. Towards a smarter hybrid energy storage system based on battery and ultracapacitor-A critical review on topology and energy management. *J Clean Prod* 2018;202:1228–40.
- [10] Trovão J, Pereirinha P, Jorge H, Antunes C. A multi-level energy management system for multi-source electric vehicles – an integrated rule-based meta-heuristic approach. *Appl Energy* 2013;105:304–18.
- [11] Zeng C, Lian H, Chen T. A wavelet transform based power allocation strategy for lithium battery and ultra capacitor hybrid vehicular power system[C]// Chinese Association of Automation. IEEE; 2017.
- [12] Li Q, Chen W. Energy management strategy for fuel cell/battery/ultracapacitor hybrid vehicle based on fuzzy logic. *Electric Power Energy Syst* 2012;43:514–25.
- [13] Gao C, Zhao J, Wu J. Optimal fuzzy logic based energy management strategy of

- battery/supercapacitor hybrid energy storage system for electric Vehicles. 2016 12th world congress on intelligent control and automation (WCICA) june 12-15. 2016 [Guilin, China].
- [14] Moura SJ, Fathy HK, Callaway DS, Stein JL. A stochastic optimal control approach for power management in plug-in hybrid electric vehicles. *IEEE Trans Contr Syst Technol* 2011;19:545–55.
- [15] Liu C, Wang Y, Chen Z. Degradation model and cycle life prediction for lithium-ion battery used in hybrid energy storage system[J]. *Energy* 2019;166:796–806.
- [16] Choi M-E, Kim S-W, Seo S-W. Energy management optimization in a battery/supercapacitor hybrid energy storage system. *IEEE Trans Smart Grid* 2012;3:463–72.
- [17] Song Z, Hofmann H, Li J. Optimization for a hybrid energy storage system in electric vehicles using dynamic programming approach. *Appl Energy* 2015;139:151–62.
- [18] Farouk O, Roes Jürgen, Angelika H. Power management optimization of an experimental fuel cell/battery/supercapacitor hybrid system[J]. *Energies* 2015;8(7):6302–27.
- [19] SONG CX, ZHOU F, XIAO F. Parameter matching of on-board hybrid energy storage system based on convex optimization method[J]. *J Journal of mechanical engineering* 2017;53(16):44–51.
- [20] Ettahir K, Boulon L, Agbossou K. Optimization-based energy management strategy for a fuel cell/battery hybrid power system[J]. *Appl Energy* 2016;163:142–53.
- [21] Borhan H, Vahidi A, Phillips AM. MPC-based energy management of a power-split hybrid electric vehicle[J]. *IEEE Trans Contr Syst Technol* 2012;20(3):593–603.
- [22] Zhu D, Xie H. Control strategy optimization of the hybrid electric bus based on remote self-learning driving cycles[C]//Vehicle power and propulsion conference. IEEE; 2008.
- [23] Dusmez S, Khaligh A. Wavelet-transform based energy and power decoupling strategy for a novel ultracapacitor-battery hybrid power-split gear powertrain [C]//Transportation Electrification Conference & Expo. IEEE; 2013.
- [24] Zhang Y, Meng D, Zhou M. Energy management of an electric city bus with battery/ultra-capacitor HESS[C]//. In: Vehicle power & propulsion conference. IEEE; 2016.
- [25] Poursamad A, Montazeri M. Design of genetic-fuzzy control strategy for parallel hybrid electric vehicles[J]. *Contr Eng Pract* 2008;16(7):861–73.
- [26] Li SG, Sharsh SM, Walsh FC. Energy and battery management of a plug-in series hybrid electric vehicle using fuzzy logic[J]. *IEEE Trans Veh Technol* 2011;60(8):3571–85.
- [27] Hu X, Johannesson L, Murgovski N, Egardt B. Longevity-conscious dimensioning and power management of the hybrid energy storage system in a fuel cell hybrid electric bus. *Appl Energy* 2015;137:913–24.
- [28] Du J, Zhang X, Wang T, et al. Battery degradation minimization oriented energy management strategy for plug-in hybrid electric bus with multi-energy storage system[J]. *Energy* 2019;175:1055–66.
- [29] Cao J, Emadi A. A new battery/ultracapacitor hybrid energy storage system for electric, hybrid, and plug-in hybrid electric vehicles. *IEEE Trans Power Electron* 2012;27:122–32.
- [30] Wang Y, Sun Z, Chen Z. Development of energy management system based on a rule-based power distribution strategy for hybrid power sources[J]. *Energy* 2019;175:1055–66.
- [31] Wu XG, Lu LG. System matching and simulation of a plug-in series hybrid electric vehicle[J]. *Automot Eng* 2013;35(07):573–582+618.
- [32] Lei ZZ, Qin D, Liu Y. Dynamic energy management for a novel hybrid electric system based on driving pattern recognition[J]. *Appl Math Model* 2017;45:940–54.
- [33] Liu GM, Ouyang MG, Lu LG. Driving range estimation for electric vehicles based on battery energy state estimation and vehicle energy consumption prediction [J]. *Automot Eng* 2014;(11):1302–9.
- [34] Zhang S, Xiong R. Adaptive energy management of a plug-in hybrid electric vehicle based on driving pattern recognition and dynamic programming. *Appl Energy* 2015;155:68–78.
- [35] Wu J. Fuzzy control strategy of parallel HEV based on driving cycle recognition. In: IEEE 7th international power electronics and motion control conference - ECCE asia; 2012. june2-5,2012, Harbin, China.
- [36] Zhang X, Wu G, Dong Z. Embedded feature-selection support vector machine for driving pattern recognition[J]. *J Franklin Inst* 2015;352(2):669–85.
- [37] Moreno J, Ortuzar ME, Dixon JW. Energy-management system for a hybrid electric vehicle, using ultracapacitors and neural networks[J]. *IEEE Trans Ind Electron* 2006;53(2):614–23.
- [38] Ridong Z, Jili T, Huiyu Z. Fuzzy optimal energy management for fuel cell and supercapacitor systems using neural network based driving pattern recognition[J]. *IEEE Trans Fuzzy Syst* 2019;27(1):45–7.
- [39] Lei ZZ, C DT, YG L. A dynamic control strategy for hybrid electric vehicles based on parameter optimization for multiple driving cycles and driving pattern recognition[J]. *Energies* 2017;10(1):54–64.
- [40] Yin AD, Zhao H, Zhou B. Driving range estimation for battery electric vehicles based on driving cycle identification[J]. *Automot Eng* 2014;(11):1310–5.
- [41] Zhou ZG. Research of PHEV energy online and realtime optimization control with self-adaptive to driving cycle. Doctor degree. Hunan: Hunan University; 2012.
- [42] Mao PL, Aggarwal RK. A novel approach to the classification of the transient phenomena in power transformers using combined wavelet transform and neural network [J]. *Power Delivery IEEE Trans* 2001;16(4):654–60.
- [43] Omar F, Gouda A. Dynamic wavelet-based tool for gearbox diagnosis. *Mech Syst Signal Process* 2012;26:190–204.
- [44] Wang H, Zhang W. Application of wavelet transform in vehicle wheel speed signal denoising[C]//. In: International conference on measuring technology & mechatronics automation. IEEE; 2009.
- [45] Wang X. Moving window-based double haar wavelet transform for image processing. *IEEE Trans Image Process* 2006;2771–9.
- [46] Dusmez S, Khaligh A. Wavelet-transform based energy and power decoupling strategy for a novel ultracapacitor-battery hybrid power-split gear powertrain [C]//. In: Transportation electrification conference & expo. IEEE; 2013.
- [47] Zhang Y, Meng D, Zhou M. Energy management of an electric city bus with battery/ultra-capacitor HESS[C]//. In: Vehicle power & propulsion conference. IEEE; 2016.
- [48] Zhang X, Mi C, Masrur A, et al. Wavelet-transform-based power management of hybrid vehicles with multiple on-board energy sources including fuel cell, battery and ultracapacitor. *Power Sources* 2008;185:1533–1543.
- [49] Ates Y, Erdinc O, Uzunoglu M. Energy management of an FC/UC hybrid vehicular power system using a combined neural network-wavelet transform based strategy. *Int J Hydrogen Energy* 2010;35:774–83.
- [50] Zhang X, Mi Chris. Vehicle power management: modeling, control and optimization. first ed. Beijing, China: China Machine Press; 2013.
- [51] Chen F. Research on transient power suppression method based on wavelet algorithm. Master degree. Nanjing: Nanjing University of Aeronautics and Astronautics; 2016.
- [52] Brahim M, Jemei S, Wimmer G. Selection of mother wavelet and decomposition level for energy management in electrical vehicles including a fuel cell. *Int J Hydrogen Energy* 2015;40:15823–33.
- [53] Ates Y, Erdinc O, Uzunoglu M. Energy management of an FC/UC hybrid vehicular power system using a combined neural network-wavelet transform based strategy. *Int J Hydrogen Energy* 2010;35:774–83.
- [54] Wang LX. A course in fuzzy systems and control. USA: Prentice-Hall, International Inc; 1999.
- [55] ZENG XH, GONG WJ. ADVISOR 2002 Simulation and redevelopment of electric vehicles. second ed. Beijing, China: China Machine Press; 2017.
- [56] Liu XT. Power system design and experimental study on composite energy storage for EV. Master degree. Guangzhou: South China University of Technology; 2016. Guangzhou.
- [57] Liang JY, Wang YR, Huang X, Geng X. Research status of balancing technique for series connected battery[J]. *Machine Building Automation* 2018;47(03):26–30.
- [58] Qian K, Zhou C, Yuan Y. Temperature effect on electric vehicle battery cycle life in vehicle-to-grid applications. *China International Conference on Electricity Distribution*; 2010.
- [59] Zhao K, Liang Z, Huang Y, et al. Research on a novel hydraulic/electric synergy bus[J]. *Energies* 2017;11(1):3.
- [60] Serrao L, Onori S, Sciarretta A, Guezennec Y, Rizzoni G. Optimal energy management of hybrid electric vehicles including battery aging. In: Proceedings of the 2011 American control conference, san francisco, CA, USA; 29 June–1 July 2011.